

Effects of Ozone Addition on Direct Initiation of Detonation in Hydrogen/Oxygen Mixtures

Haiyue Li ^{a,b}, Wenkai Liang ^{a,c}, Chung K. Law ^{c,a}

^a Center for Combustion Energy, Tsinghua University, Beijing 100084, China

^b State Key Laboratory for Turbulence and Complex Systems, College of Engineering, Peking University, Beijing 100871, China

^c Department of Mechanical and Aerospace Engineering, Princeton University, Princeton, NJ 08544, USA

1 Introduction

Due to the advantages such as high thermal efficiency and geometric simplicity, detonation engines have become a promising application in advanced propulsion, where stable and manipulable detonation initiation and propagation are required. Therefore, smooth and efficient detonation initiation under detonation-engine relevant conditions receives increasing attentions. From the fundamental aspect, successful detonation initiation can be realized by either the direct initiation with a massive energy source deposited locally, or the process of deflagration to detonation transition (DDT). Understanding the corresponding dynamic behaviors is helpful for providing technical guidance on the design of detonation initiation devices.

Being one of the strongest oxidizers and the longest-lived excited species generated from non-equilibrium plasma, ozone has been reported to significantly enhance various types of combustion phenomena, such as ignition, flame propagation, and detonation initiation. Particularly, the application of ozone addition into the H_2/O_2 combustion system has received considerable attention, due to its kinetic simplicity as well as practical relevance to aero-propulsion, explosion safety, and reduced carbon emission. For the $H_2/O_2/O_3$ system, explosion [1], ignition [2, 3] and flame propagation [2], spontaneous detonation initiation [3, 4], stability[5] and cellular structure [5, 6] have been reported in previous studies. It is found that ozone chemistry introduces an additional low-temperature regime in ignition, flame and detonation, and as such combustion phenomena occurring in $H_2/O_2/O_3$ mixtures are generally featured by two-step heat release respectively featured by oxidation processes with ozone and oxygen.

We further note that it is still not clear on how ozone chemistry influences direct detonation initiation, which is an important approach to realizing the desired initiation properties in the detonation engine relevant conditions. This gap motivates the present study on both the steady detonation structure and transient dynamic behaviors during direct detonation initiation affected by ozone addition. The remaining of this paper proceeds as follows: in Section 2 numerical models and methods are presented; Correspondence to: lihaiyue@pku.edu.cn; lihaiyue@mails.tsinghua.edu.cn (Haiyue Li)

in Section 3 steady detonation structure with different amounts of ozone addition is discussed; in Section 4 the dynamic behaviors during direct detonation initiation are respectively examined in planar and spherical configurations; and in Section 5 the closing comments are provided.

2 Numerical Model and Methods

We consider both the steady ZND structure and transient evolution of direct detonation initiation in homogeneous $\text{H}_2/\text{O}_2/\text{O}_3$ mixtures initially at $T_0 = 300$ K and $P_0 = 1$ atm, $\phi = 1$. Following [1], the concentration of the $\text{H}_2\text{-O}_2\text{-O}_3$ mixture is defined as $\phi(2+\alpha)\text{H}_2+(1-\alpha)\text{O}_2+\alpha\text{O}_3$, where the extra O in ozone is taken into account in the equivalence ratio, ϕ . Note that α indicates the percentage of ozone in the oxidizer, instead of the ozone fraction in the unburnt gaseous mixtures [3]. The detailed $\text{H}_2\text{-O}_2$ mechanism developed by Burke et al. [7] together with the ozone sub-mechanism [8] is adopted.

The ZND computation is carried out using a modified version of the CalTech Shock and Detonation Toolbox [9]. Cantera [10] integrated with MATLAB and Python is used in the chemical kinetics simulations. The transient detonation initiation is numerically studied by the A-SURF code, with the CHEMKIN packages [11] incorporated to calculate the transport and thermodynamic properties as well as the reaction rates. A-SURF has been demonstrated to accurately resolve ignition, flame propagation, autoignition and detonation [12-14]. Details of the governing equations and numerical methods of A-SURF are given in [12-14]. Dynamical adaptive mesh is used to accurately resolve the flame front, which is fully covered by the finest mesh size of $8\ \mu\text{m}$, with the time step Δt smaller than 4×10^{-10} s and thereby the Courant-Friedrichs-Lewy (CFL) number is always equal or less than 0.25.

The Taylor-Sedov [15, 16] blast wave model is used as the initial condition in $0 < x < 1$ cm to simulate the transient process of direct detonation initiation and propagation in the computational domain $0 \leq x \leq L = 10$ cm. Note that a cutoff temperature of 10000 K and the corresponding state parameters are applied in all simulations to ensure meaningful comparisons. The subsequent decay of the blast wave with chemical reaction is governed by Euler equations. Adiabatic wall boundary conditions (zero flow velocity, and zero temperature and mass fraction gradients for all species) are imposed at both ends.

3 Steady ZND Structure

To understand the role of ozone chemistry in detonation, the steady structure with different amounts of ozone addition in stoichiometric is first numerically studied by the Zeldovich-von Neumann-Doring (ZND) model. Thermicity profiles with different ozone addition are plotted in Fig. 1 (a). It is seen that the thermicity profiles responses differently to the ozone fraction in the oxidizer. Small amounts of ozone fraction ($\alpha = 0, 0.001, 0.01$) greatly reduces the induction length while almost does not change the maximum thermicity. However, for large amounts of ozone fraction ($\alpha = 0.1, 0.2$) an additional thermicity peak appears at smaller post-shock distance, and the first/second thermicity peak respectively increases/decreases with the ozone fraction in the oxidizer, α .

To further understand the underlying chemical mechanisms for the above double-peak structure, net progress rates for key chemical pathway for $\alpha = 0.1$ is shown in Fig. 1(b). It is found that ozone chemistry results in an additional peak at smaller post-shock distance in the thermicity profile. The first-stage heat release is primarily contributed by the reaction between ozone and H, $\text{O}_3+\text{H}=\text{O}_2+\text{OH}$ (R31), whereas a series of ozone reactions occurring in this stage is first triggered by ozone decomposition reaction $\text{O}_3+\text{M}=\text{O}_2+\text{O}+\text{M}$ (R28). Meanwhile, the second stage heat release is kinetically interpreted by hydrogen/oxygen chemistry. In this stage $\text{H}_2 + \text{OH} = \text{H}_2\text{O} + \text{H}$ (R4), $\text{H} + \text{O}_2 = \text{O} + \text{OH}$ (R1) and $\text{O} + \text{H}_2 = \text{H} + \text{OH}$ (R3) are the top three reactions with the largest net rates of progress.

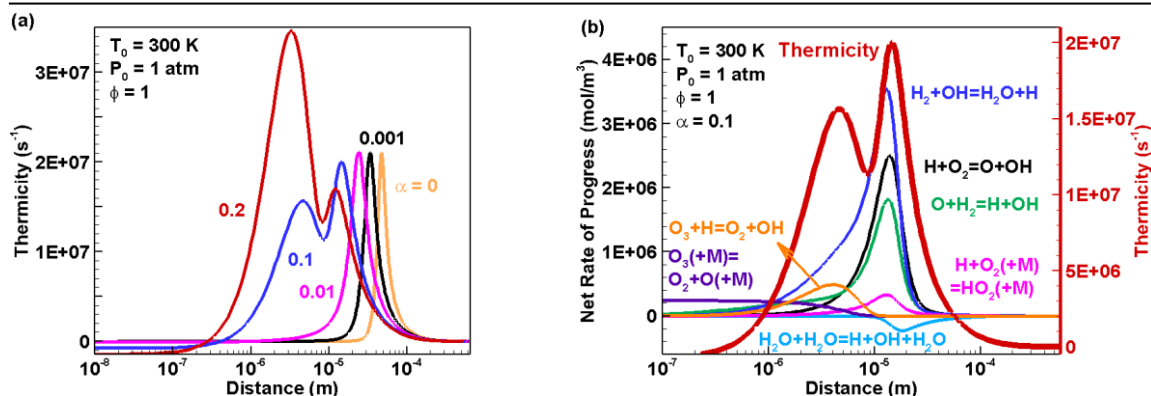


Figure 1: (a) Profiles of thermicity for $\alpha = 0, 0.001, 0.01, 0.1, 0.2$ (0, 333, 3322, 32258, 62500 ppm O₃); (b) Profiles of net rate of progress for key reactions and thermicity in the steady ZND structure for $\alpha = 0.1$ in homogeneous H₂/O₂/O₃ mixtures at $T_0 = 300$ K and $P_0 = 1$ atm, $\phi = 1$.

4 Transient Evolution of Direct Detonation Initiation

4.1 Direct Initiation of a Planar Detonation

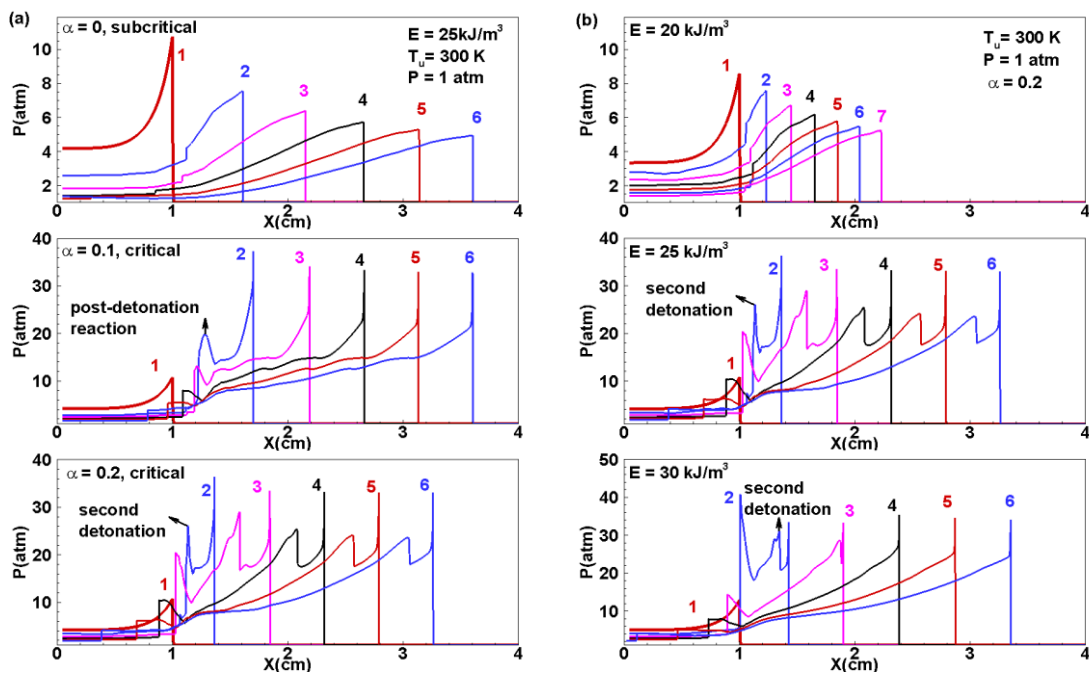


Figure 2: Temporal evolution of pressure distribution during direct planar detonation initiation and propagation in stoichiometric H₂/O₂/O₃ mixtures initially at $T_0 = 300$ K, $P = 1$ atm, $\phi = 1$, (a) initiation energy $E = 25$ kJ/m³ with different ozone fraction and (b) $\alpha = 0.2$ with different initiation energy.

Recognizing the significant influence of curvature on direct detonation initiation, planar and spherical configurations are respectively examined. We first consider different dynamic behaviors in direct initiation of a planar detonation. Fig. 2(a) plots the temporal evolution of pressure distribution for three cases with the same initiation energy $E = 25$ kJ/m³ and different ozone fraction in the oxidizer, $\alpha = 0, 0.1, 0.2$. The ozone-free case ($\alpha = 0$) corresponds to the subcritical regime, indicating that an instant detonation wave fails to form in this referee condition without ozone addition. Meanwhile, successful

detonation initiation is observed in cases with ozone addition ($\alpha = 0.1$ and $\alpha = 0.2$), which also implies that ozone addition reduces the critical initiation energy and enhance direct detonation initiation.

Particularly, an additional reaction front is observed to form behind the detonation wave in cases with ozone addition ($\alpha = 0.1$ and $\alpha = 0.2$). This behavior is significantly different from the conventional dynamics for direct detonation initiation, and is caused by the two-step heat release occurring in $\text{H}_2/\text{O}_2/\text{O}_3$ mixtures behind the shock. Specifically, the first-stage occurs first couples with the leading shock and forms the leading detonation wave, whereas the second-stage heat release then occurs and leads to post-detonation reaction. For $\alpha = 0.1$ this post-detonation reaction gradually quenches, whereas for $\alpha = 0.2$ this reaction front also develops into a detonation wave and then degenerates in to a shock wave propagating behind the leading one.

Fig. 2(b) plots the temporal evolution of pressure distribution for three demonstrative cases with the same ozone fraction in the oxidizer, $\alpha = 0.2$ and different initiation energy $E = 20, 25, 30 \text{ kJ/m}^3$. For $E = 20 \text{ kJ/m}^3$ the heat release and propagating blast wave fail to couple to form a detonation wave. For $E = 25 \text{ kJ/m}^3$ the above-mentioned double-shock structure is observed. For $E = 30 \text{ kJ/m}^3$ double-shock structure appears and then the second shock rapidly catches up the leading one. Such different dynamics can be attributed to the different energy density levels. As the energy density of the mixtures behind the leading detonation wave increase, the second detonation wave tends to propagate at larger velocity.

4.2 Direct Initiation of a Spherical Detonation

We next study the role of ozone addition on dynamic behaviors during direct initiation of a spherical detonation. Figure 3 plots the spatial change of leading shock velocity with different initiation energy in the cases without and with ozone addition ($\alpha = 0$ and 0.1). In the ozone-free condition ($\alpha = 0$), four cases with initiation energy $E_s = 10.5, 10.6, 10.7$ and 10.8 J have been considered. The temporal changes of leading shock velocity exhibit three modes, specifically: (1) the leading shock velocity decreases monotonically with its location for the case of $E_s = 10.5 \text{ J}$; (2) this velocity slightly increases then decreases for cases of $E_s = 10.6$ and 10.7 J ; (3) an overdriven detonation is successfully generated when the initial energy increases to 10.8 J . In the five cases with ozone addition ($\alpha = 0.1$) initiated by different energy $E_s = 6.875, 7.19, 7.35, 7.36$, and 7.43 J , an additional dynamic mode is observed in the case of $E_s = 7.36 \text{ J}$, where the leading shock velocity step increases around $x = 1.35 \text{ cm}$ and then gradually decreases, until an over-driven detonation first appears at around $x = 1.65 \text{ cm}$.

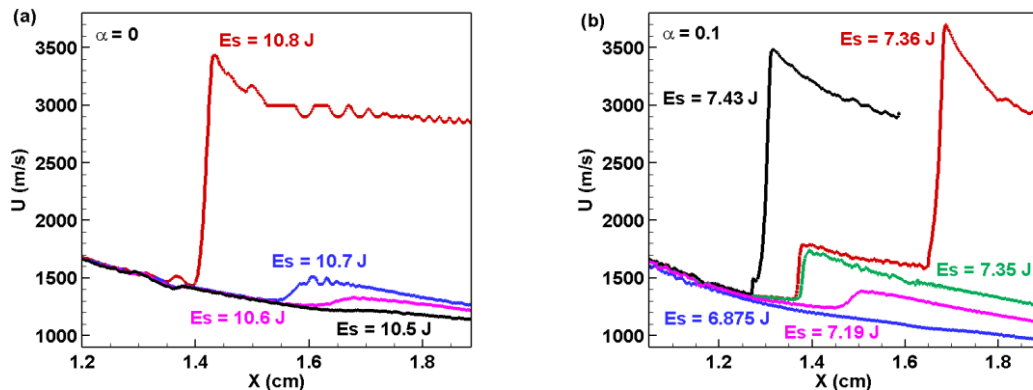


Figure 3: Effect of initiation energy on the leading shock velocity during direct detonation initiation in stoichiometric $\text{H}_2/\text{O}_2/\text{O}_3$ mixtures initially at $T_0 = 300 \text{ K}$ and $P_0 = 1 \text{ atm}$, $\phi = 1$, (a) $\alpha = 0$ and (b) $\alpha = 0.1$ with different initiation energy.

Then the temporal evolutions of pressure distribution for the above-mentioned cases have been examined. Results for ozone-free cases are shown in Fig. 4(a). For $E_s = 10.5 \text{ J}$, the emerging reaction wave immediately decays and always falls behind the leading shock. For $E_s = 10.6 \text{ J}$, the post-shock reaction catches up the leading shock wave, but fails to evolve into a detonation wave due to the influence of curvature loss. Nevertheless, the interaction between post-shock reaction and leading shock leads to a

step increase in leading shock velocity shown in Fig. 3(a). For $E_s = 10.8$ J the heat release and leading shock successfully couples into a detonation. Fig. 4(b) plots the results with ozone addition ($\alpha = 0.1$), and the above-mentioned dynamic behaviors for initiation failure/success around the critical energy are respectively observed for $E_s = 7.35$ J and 7.43 J. As for $E_s = 7.36$ J, a detonation wave first fails to form around $x = 1.35$ cm (Lines #3 and #4), and then develops at a larger distance ($x = 1.65$ cm) with less curvature loss (Line # 5 and #6). Such re-initiation process explains the over-driven detonation development after the step increase in leading shock velocity shown in Fig. 3(b).

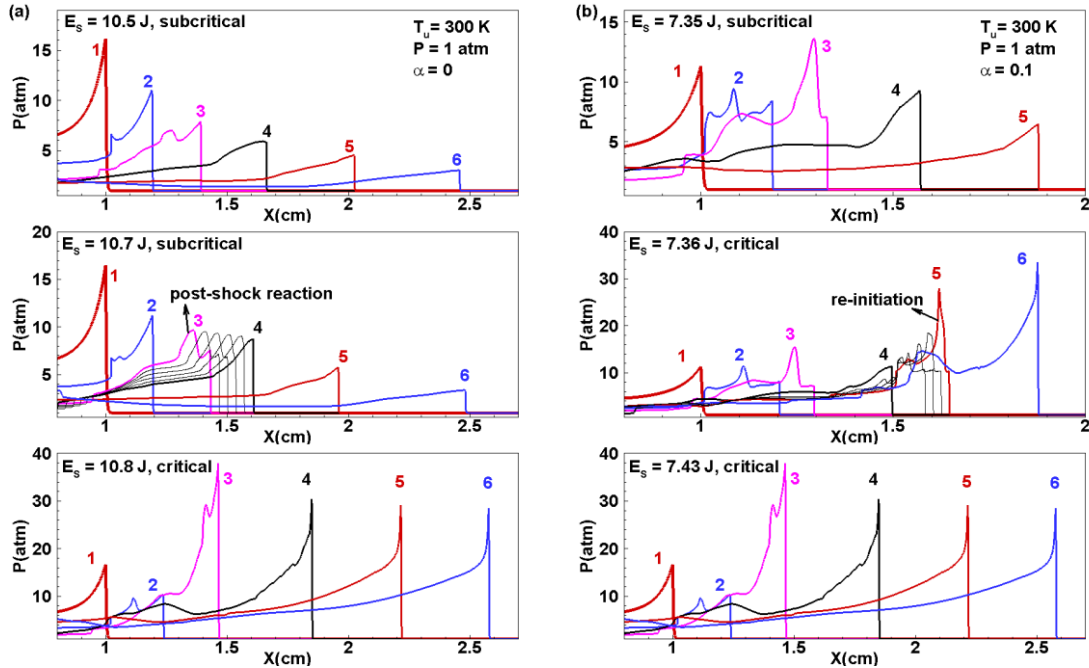


Figure 4: Temporal evolution of pressure distribution during direct spherical detonation initiation and propagation in stoichiometric $H_2/O_2/O_3$ mixtures initially at $T_0 = 300$ K, $P = 1$ atm, $\phi = 1$, (a) $\alpha = 0$ and (b) $\alpha = 0.1$ with different initiation energy.

5 Conclusions

This study computationally investigates how ozone addition influence direct detonation initiation in stoichiometric $H_2/O_2/O_3$ mixtures. Substantial ozone addition is found to result in an additional thermicity peak in the steady ZND structure, and as such introduces different dynamic behaviors (e.g., post-shock reaction, double-detonation structure, and re-initiation) during transient process of direct detonation initiation and propagation. Major conclusions are summarized in the following:

1. Ozone addition significantly modifies the steady ZND structure of the stoichiometric H_2/O_2 detonation. The influence of ozone chemistry behaves differently at various amounts of ozone fractions. Specifically, small amounts of ozone addition significantly reduce the induction length without changing the thermicity, whereas large amounts of ozone result in an additional peak at smaller post-shock distance. According to chemical pathway analysis, this additional peak is primarily contributed by the reaction between ozone and H, $O_3+H=O_2+OH$ (R31), and a series of ozone reactions are first triggered by ozone decomposition, $O_3+M=O_2+O+M$ (R28).
2. Corresponding to the double peaks in the steady ZND structure, an additional post-shock reaction wave may appear with various dynamic behaviors in the transient process of direct detonation initiation. In planar configuration, such additional post-shock reaction and subsequent detonation initiation occur as the initiation energy further increases above the critical value. The latter shock wave may rapidly decay, propagate behind or catch up the leading one with different initiation energy and ozone fraction.

In the spherical configuration with curvature loss, a leading shock failing to couple into a detonation wave is observed to re-initiate behind when the initiation energy is just over the critical energy. It is also noted that ozone addition greatly reduces the critical initiation energy in direct detonation initiation.

References

- [1] W. Liang, Y. Wang, and C.K. Law, Role of ozone doping in the explosion limits of hydrogen-oxygen mixtures: Multiplicity and catalyticity, *Combustion and Flame* 205 (2019) 7-10
- [2] H. Li, W. Liang, and C.K. Law, Role of ozone addition on premixed hydrogen/oxygen flames: Multi-zone structure and multi-regime dynamics, *Combustion and Flame* (2022)
- [3] H. Li, W. Liang, and C.K. Law, Facilitated ignition and detonation initiation of hydrogen-oxygen mixtures by ozone doping, *Combustion and Flame* 246 (2022) 112474
- [4] W. Han, W. Liang, C. Wang, J.X. Wen, and C.K. Law, Spontaneous initiation and development of hydrogen–oxygen detonation with ozone sensitization, *Proceedings of the Combustion Institute* 38 (2021) 3575-3583
- [5] W. Han, J. Huang, and C. Wang, Pulsating and cellular instabilities of hydrogen–oxygen detonations with ozone sensitization, *Physics of Fluids* 33 (2021) 076113
- [6] J. Crane, X. Shi, A.V. Singh, Y. Tao, and H. Wang, Isolating the effect of induction length on detonation structure: Hydrogen–oxygen detonation promoted by ozone, *Combustion and Flame* 200 (2019) 44-52
- [7] M.P. Burke, M. Chaos, Y. Ju, F.L. Dryer, and S.J. Klippenstein, Comprehensive H₂/O₂ kinetic model for high-pressure combustion, *International Journal of Chemical Kinetics* 44 (2012) 444-474
- [8] H. Zhao, X. Yang, and Y. Ju, Kinetic studies of ozone assisted low temperature oxidation of dimethyl ether in a flow reactor using molecular-beam mass spectrometry, *Combustion and Flame* 173 (2016) 187-194
- [9] S. Browne, J. Ziegler, J.E. Shepherd, Numerical Solution Methods for Shock and Detonation Jump Conditions, California Institute of Technology, 2018 GALCIT Report FM2006.006 - R3
- [10] David G. Goodwin, Raymond L. Speth, Harry K. Moffat, and Bryan W. Weber, Cantera: An object-oriented software toolkit for chemical kinetics, thermodynamics, and transport processes. <https://www.cantera.org>, 2021. Version 2.5.1. doi:10.5281/zenodo.4527812
- [11] R.J. Kee, G. Dixon-Lewis, J. Warnatz, M.E. Coltrin, and J.A. Miller, A Fortran computer code package for the evaluation of gas-phase multicomponent transport properties, Sandia National Laboratories Report SAND86-8246 13 (1986) 80401-1887
- [12] Z. Chen, M. Burke, and Y. Ju, Effects of Lewis number and ignition energy on the determination of laminar flame speed using propagating spherical flames, *Proceedings of the Combustion Institute* 32 (2009) 1253-1260
- [13] Z. Chen, Effects of radiation and compression on propagating spherical flames of methane/air mixtures near the lean flammability limit, *Combustion and Flame* 157 (2010) 2267-2276
- [14] P. Dai, Z. Chen, S. Chen, and Y. Ju, Numerical experiments on reaction front propagation in n-heptane/air mixture with temperature gradient, *Proceedings of the Combustion Institute* 35 (2015) 3045-3052
- [15] G.I. Taylor, The formation of a blast wave by a very intense explosion, *Proceedings of the Royal Society of London* 201 (1950) 159-174
- [16] L.I. Sedov, M. Friedman, and R. Street, Similarity and dimensional methods in mechanics, *Journal of Applied Mechanics* 1982 (1959) 355-358